TiN Nanofibers: A New Material with High Conductivity and Transmittance for Transparent Conductive Electrodes

Heping Li, Wei Pan, Wei Zhang, Siya Huang, and Hui Wu*

Motivated by the rising cost of tin-doped indium oxide (ITO), the search for new transparent electrode materials to replace ITO is ongoing. TiN exhibits high electric conductivity, however, it is generally non-transparent. Here, nanostructured TiN fiber patterns are synthesized on quartz glass and the resulting materials have a combination of high electric conductivity and optical transparency. A low sheet resistance of 15.8 Ohm sq^{-1} at 84% transparency is achieved on TiN nanofiber arrayed quartz glass. The achievements show a successful integration of electric and optical properties in ceramic nanofibers and provide a method for finding new materials to replace traditional ITO-based transparent electrodes.

1. Introduction

Titanium nitride (TiN) has been intensely studied for applications including wear- and corrosion-resistant coatings and cutting tools due to its high melting point, high hardness and high thermal stability. Moreover, TiN materials hold potential for wide applications in electric devices due to its high electric conductivity and chemical stability.[1] Traditionally, TiN ceramics have not been integrated in optoelectric devices due to their opaque nature. Here, we report the successful fabrication of transparent conducting TiN thin films by nanoscale materials designing and processing. For the first time, TiN nanofibers were synthesized and assembled into oriented patterns by a simple and scalable electrospinning method on the quartz glass. The TiN nanofiber networks show a sheet resistance of 15.8 to 670 Ohm sq^{-1} and transmittance of ≈84% to 97%, which is comparable to commercial tin-doped indium oxide (ITO) thin film transparent electrodes.

Transparent electrodes are widely used as the fundamental component in many optoelectronic devices including displays, solar cells, organic light-emitting diodes, and smart windows.[2,3] Most important functions of transparent electrodes are electric conductivity and optical transmittance. Currently, ITO is the most commonly used transparent electrode because of its high electric conductivity and high transmittance. However, its rising cost due to the low abundance of indium severely limits its applications in future large-area optoelectronic devices. Therefore, there has been much effort both in industry and in academia to find a replacement for ITO.[4] Emerging candidates are conducting polymers, carbon nanotubes, graphene, and metallic nanowires.[5–9] A graphene-based thin film has been assembled onto polymer nanofibers.[10] However, the sheet resistance of 8.6×10^3 Ohm sq^{-1} at 88% light transmittance is too high. More conductive carbon nanotube films with the sheet resistance of 1000 Ohm sq^{-1} at 85% transparency have been developed as transparent electrode.[11] However, their performance still lags behind those of ITO films. Along the same lines, graphene with competitive performance fabricated by chemical vapor deposition (CVD) was put forward as candidate materials.[5,12,13] High-quality graphene film fabrication is still under investigation, and moreover, the CVD method also faces challenges in large-scale production at low cost. A. recent report by the Yi Cui group synthesized metal nanowire network with 50 Ohm sq^{-1} at 90% transparency as transparent electrode.[13] Whereas, metal nanowire is more active than bulk metal materials due to its quantum size effect and high aspect ratios. Whether the chemical stability of these metal nanowire network could hold the line with high performance during its actual applications remains a question. Thus, our attention has been focused on a new domain-TiN, concerning its low resistivity and high chemical durability.

2. Results and Discussion

In a typical experimental procedure, TiN nanofibers were prepared with three steps: 1) Fabrication of precursor composite nanofibers by electrospinning of poly (vinyl pyrrolidone) (PVP) and tetrabutyl titanate solutions. 2) Calcination of the precursor nanofibers in air at 500 °C for 2 h to thoroughly remove organic components. Anatase TiO_2 nanofibers were synthesized in this step, as confirmed by X-ray diffraction (Supporting Information Figure S1). 3) Conversion of TiO_2 nanofibers into TiN nanofibers by ammonification at high temperature.

The corresponding phase transformations were monitored using X-ray diffraction (XRD, **Figure 1**a). The nanofibers are found to be mainly composed of anatase and rutile phases when the calcination temperature is below 600 °C. With temperature increasing to 700 °C, reflection peaks indexed to face-centered cubic structured TiN appear. Above 800 °C,

H. Li, Prof. W. Pan, W. Zhang, S. Huang, Dr. H. Wu
State Key Laboratory of New Ceramic and Fine Processing
Department of Materials Science and Engineering
Tsinghua University
Beijing 100084, P. R. China
E-mail: panw@mail.tsinghua.edu.cn

DOI: 10.1002/adfm.201200996

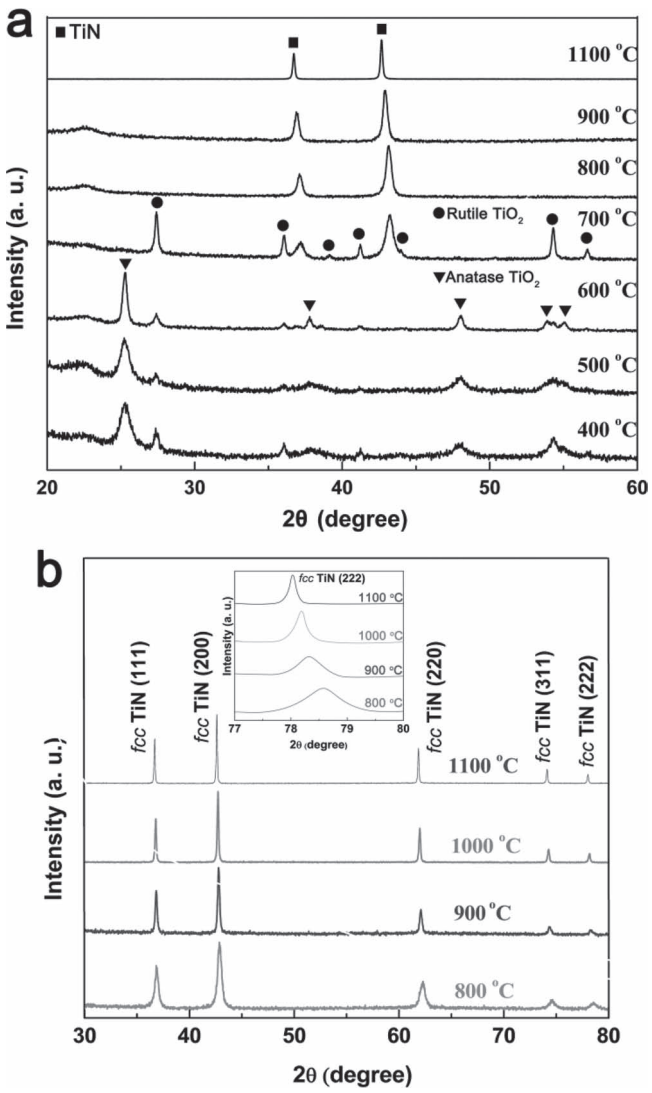

Figure 1. a) XRD patterns of the nanofibers calcined under NH_3 flow at different temperatures for 4 h. b) XRD patterns of the TiN nanofibers calcinated under NH_3 flow at temperatures from 800 to 1100 °C for 4 h and the up inset is the step-scanning XRD of these TiN nanofibers.

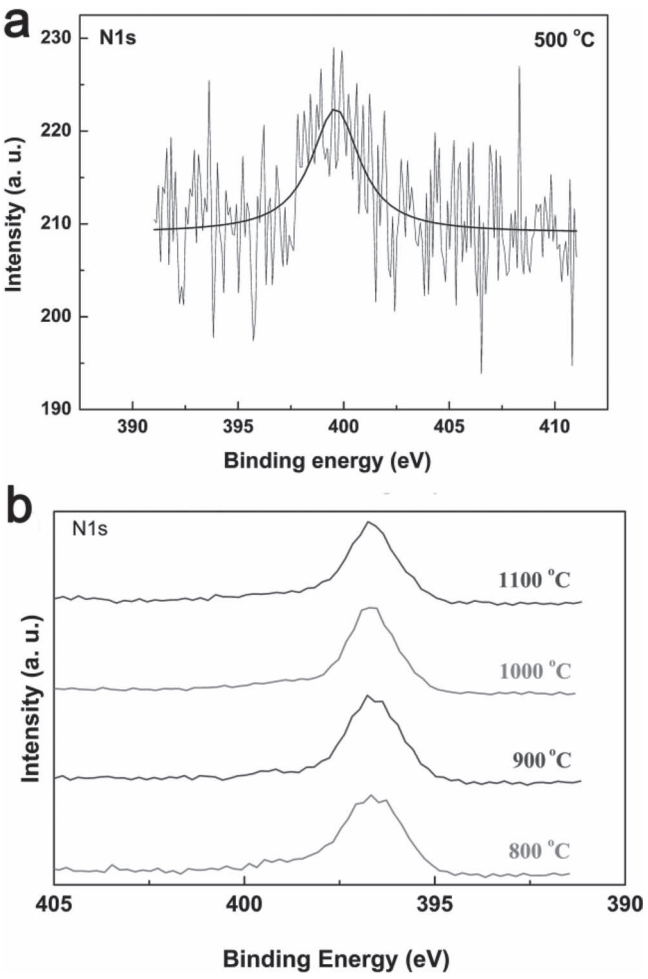

Figure 2. a) N1s XPS spectra of the nanofibers calcined under NH_3 flow at 500 °C for 4 h. b) N1s XPS spectra of TiN nanofibers calcined under NH_3 flow at temperatures from 800 to 1100 °C for 4 h.

pure TiN phase is observed in the calcined nanofibers, and no other impurities could be indexed from the as-synthesized products, which is in accord with the energy-dispersive X-ray spectroscopy result (Supporting Information Figure S2). More particular XRD spectra of TiN nanofiber obtained after high temperatures annealing is shown in Figure 1b. From the XRD analysis, TiN nanofibers are well crystallized when calcined at temperatures higher than 800 °C. Moreover, as revealed in the inset of Figure 1b, with the calcination temperature going up, the <222> peak of TiN shifts to the smaller 2θ angle direction, indicating the increase of lattice constant. Besides XRD, X-ray photoelectron spectroscopy (XPS) has also been adopted to analyze the chemical state and concentration of the N atom in the nanofibers. When annealed at 500 °C in ammonia atmosphere, the N1s spectra shows a clear N1s bond energy around 400 eV (**Figure 2**a), suggesting the formation of Ti-O-N bonding.[15–17] Whereas, when annealed at temperatures above 800 °C, the N1s bond energy decreases to 396 eV in Figure 2b. This is due to the N substituting O atom in the crystal lattice and forming the Ti-N bonding.[15,18,19] From 800 to 1100 °C, the atomic concentration ratios of N/Ti were calculated to be 1.03, 1.11, 1.20, 1.26 from the XPS data, respectively. Thus, the increase of lattice parameter as mentioned above (Figure 1b) is attributed to the increasing amount of N atom existing as interstitial atoms in the TiN lattice forming nonstoichiometric TiN_x.

Transmission electron microscopy (TEM) images of TiN nanofibers sintered in ammonia atmosphere at temperatures ranging from 800 to 1100 °C are displayed in **Figure 3**a–d, which demonstrate that diameter of the nanofiber is uniform throughout the entire length and the grain is growing as calcination temperature increases. After calcined at 1100 °C, the gain size is so large that the nanofiber demonstrates a necklace structure. The corresponding electron diffraction patterns (Supporting Information Figure S3) and high-resolution (HR) TEM images (Figure 3e,f) indicate that the structure of nanofibers is polycrystalline constituting of fine grains of 10–20 nm after calcination at 800 °C and the grain size increases to 50–100 nm when

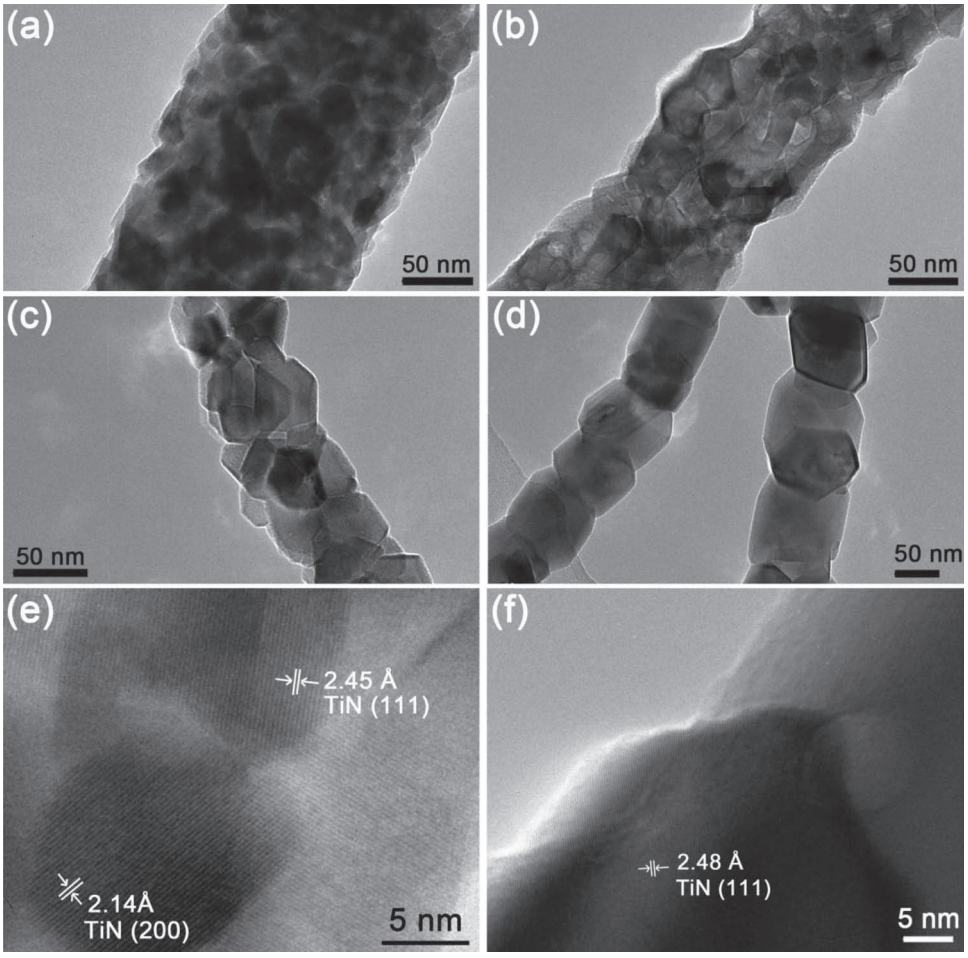

Figure 3. TEM images of the TiN nanofibers calcined under NH_3 flow for 4 h at different temperatures: a) 800 °C; b) 900 °C; c) 1000 °C; and d) 1100 °C. e) HRTEM image in (a). f) HRTEM image in (d).

temperature goes up to 1100 °C. The increase grain size and variety of N/Ti ratios lead to apparent color changes of the TiN_x nanofiber from dark cyan to reddish-brown, then from reddish-brown to dark yellow, and finally to golden yellow as ammonfication temperature inceasing (Supporting Information Figure S4).

Figure 4a shows an SEM image of the random distributed TiN nanofiber networks, which were calcined at 1100 °C in ammonia atmosphere. Clearly, the nanofibers remained intact and continuous with length up to several millimeters (Figure 4a). It can be more clearly seen from Figure 4b that the surface of TiN nanofibers is rough as they were calcined at 1100 °C due to the grain growth. While when calcined at 800 °C, TiN nanofibers obtained with an average diameter of 120 nm, show the relatively smooth surface (Figure 4c). Besides random nanofiber networks, electrospinning can also provide a facile process to assemble nanofibers into aligned arrays.[20] By using a modified fiber collector, nanofiber arrays could be assembled as grid-patterned nanofiber network as shown in Figure 4d.

It is well known that TiN is a good electric conductor due to its metallic bond. By taking advantage of easily fiber patterning with electrospinning, we are able to investigate the electric transport properties of single TiN nanofiber with controlled orientation. In a typical measurement, gold electrodes were deposited on the two ends of a single TiN nanofiber with length of 500 μm (up inset of **Figure 5**a). Figure 5a shows the current-voltage (*I*–*V*) curve through single TiN nanofiber calcined at different temperatures ranging from 800 to 1000 °C. The linear IV curve indicates a metallic conducting characteristic of the TiN nanofibers. It is found that the current through nanofibers is remarkably debased with the increase of calcination temperature. This is maybe caused by the change of N content in the obtained TiN nanofibers. It is well accepted that TiN, holding both the covalent nature of Ti-N bonds and metallic bonds, possesses a blend of ceramic and metallic properties. If the atom ratio of N/Ti is close to 1:1, TiN will exhibit metallic character. On the contrary, if the atom ratio of N/Ti is larger than 1:1, TiN_x ($x > 1$) will exhibit the typical properties of non-metallic compounds. As analyzed by the foregoing XPS data, the concentration of N atom in the obtained TiN nanofibers increases with calcination temperature climbing. Accordingly, the decrease conductivity of the TiN nanofibers given in Figure 5a is reasonable. The relation between the electric conductivity and the ammonification temperature is plotted in Figure 5b. Results show that the conductivity of the TiN nanofiber was calculated to be 121.1, 49.1 and 29.5 S cm^{-1} at

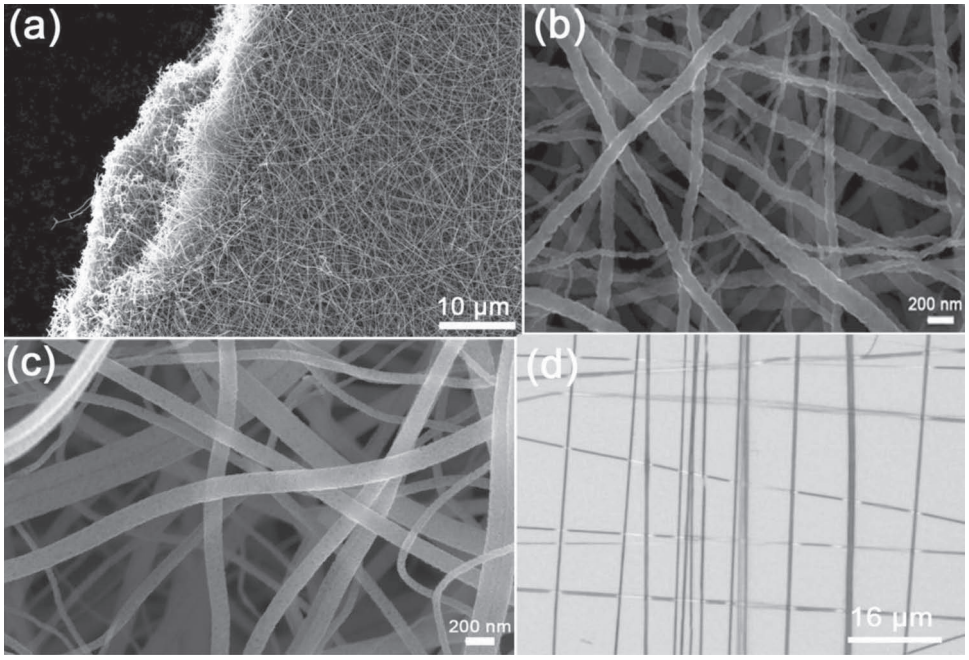

Figure 4. a) 2000 diameter and b) 100 000 diameter SEM image of TiN nanofibers calcined under NH_3 flow at 1100 °C for 4 h. c) 100 000 diameter SEM image of TiN nanofibers calcined under NH_3 flow at 800 °C for 4 h. d) Laser microscope image of assembled grid-patterned precursor nanofibers.

sintering temperature of 800 °C, 900 °C and 1000 °C. The high conductivity (≈121.1 S cm^{-1}) of the TiN nanofibers sintered at 800 °C is much larger than that of electrospun ZnO nanofiber (≈6.0×10^{-6} S cm^{-1}) and ITO nanofibers (≈1.0 S cm^{-1}) reported before[21,22] and even surpasses that of Ag-ZnO nanofiber with 50.0 at.% Ag (115 S cm^{-1}) and carbon nanofiber (≈20–30 S cm^{-1}).[21,23] High electric conductivity promotes TiN nanofibers to be a promising alternative to carbon based materials such as carbon nanofibers and nanotubes in electronic devices.

Electrospun TiN nanofiber networks on quartz glass also exhibit high optical transparency, which boost the application of TiN nanofibers as a new kind of high performance transparent electrode. The grid-patterned TiN nanofiber network was assembled on the quartz glass (as shown schematically in the lower part of **Figure 6**). After calcination in air and ammonia atmosphere, TiN nanofibers adhere to the quartz glass surface firmly owing to sintering between fiber and glass. Benefited from the extremely high aspect ratios of electrospun nanofibers, the charge carriers can transfer along the fibers with little junction scattering and accordingly enhance the surface conductance.[24] The density of TiN nanofiber networks can be easily controlled by adjusting the electrospinning deposition cycle index. As observed in Figure 6, the TiN nanofiber network shows high optical transmittance in the visible and near-infrared ranges. TiN networks assembled with different electrospinning cycle index exhibit dissimilar transparencies. With electrospinning cycle index increasing, the optical transmittance visibly decreases from 97% to 84%. The optical transmittance of the TiN nanofiber networks is compared with that of the dense TiN film prepared by spin coating using the same electrospinning precursor solution. Even though light scattering exists in the TiN nanofibers system, the optical transmittance of the TiN nanofiber networks is about three times higher than that of the TiN film (Supporting Information Figure S5), which may be attributed to the hollow space presented in nanofiber networks. These results are in consistent with observations in carbon nanotube networks,[25] silver nanowire networks,[26] copper nanowire networks[13] and indium oxide nanofiber networks.[27] According to the literatures,[13,28] on the other hand, the light scattering by the nanofibers is profitable for some devices, such as solar cells, where scattering is preferred. The enhanced scattering of light allows for higher solar cell efficiencies by providing better absorption. Backtrack to the performance of TiN nanofiber networks as transparent electrode, the sheet resistance measurements of these networks mentioned above were carried out by a four-probe method to avoid contact resistance between test electrodes and TiN nanofibers. The results are displayed in **Figure 7**a. The sheet resistance decreases sharply as the density of TiN nanofibers increases. The corresponding sheet conductance as a function of electrospinning cycles has been plotted in Supporting Information Figure S6. When the electrospinning cycles are less than three, the sheet conductance increases progressively. As the electrospinning cycles increase from three to four, the sheet conductance increases abruptly, which is caused by a near-percolative nanofiber density following the percolation behavior of one-dimensional stick systems.[10] The lowest sheet resistance value 15.8 Ohm sq^{-1} was obtained with 4 electrospinning cycles. When electrospun TiN nanofiber network was deposited with different cycles, surface resistances of 670 Ohm sq^{-1}, 452 Ohm sq^{-1}, 193 Ohm sq^{-1}, and 15.8 Ohm sq^{-1} were achieved at ≈97%, ≈95%, ≈93%, and ≈84% transparency, respectively, as shown in Figure 7b.

One problem that arises in the present TiN nanofiber networks is the poor flexibility. One suggestion for solving this

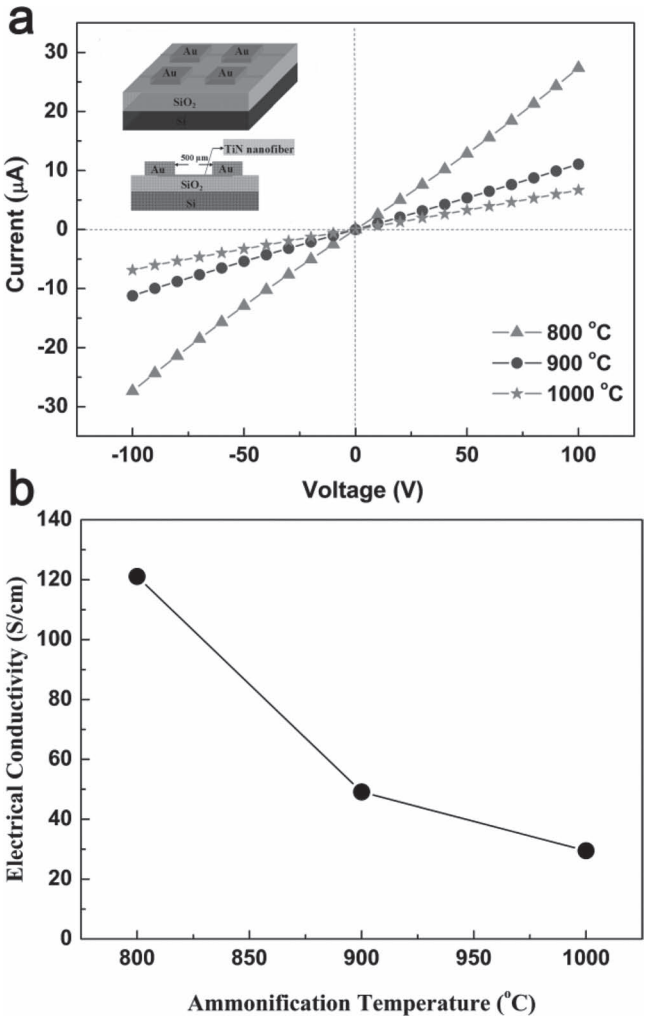

Figure 5. a) *I–V* characteristics of TiN nanofibers calcined under NH_3 flow at temperatures from 800 to 1000 °C for 4 h. The inset is the patterning Au electrodes on the nanofibers for device testing. b) The relationship between the electrical conductivity and the ammonification temperature of TiN nanofibers.

issue is to transfer the prepared TiN nanofiber networks to flexible substrates such as poly(dimethysiloxane) (PDMS) or poly(ethylene terephthlate) (PET) film by dispersion of TiN nanofibers in methanol solution to form TiN nanofiber ink and following the slot die or graver coating process.[28] Thus, high electrical conductivity combining with high optical transparency, low-cost and easy scale-up, will enable TiN nanofiber network to be a competitive candidate material for transparent electrode.

3. Conclusions

In summary, we have successfully synthesized high-quality TiN nanofibers by the combination of electrospinning and ammonification process. A single TiN nanofiber shows a linear *I–V* curve, with the conductivity up to 121.1 S cm^{-1}. The TiN nanofiber networks exhibit high electrical conductivity and high optical transmittance. A sheet resistance of 15.8 Ohm sq^{-1} has been achieved at 84% transmittance.

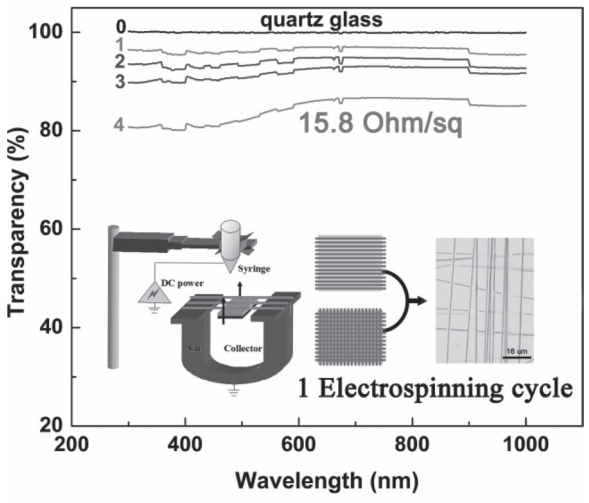

Figure 6. Transmittance spectrum of TiN nanofiber networks with different electrospinning cycles. The inset shows the set up for collecting well-aligned electrospun nanofibers.

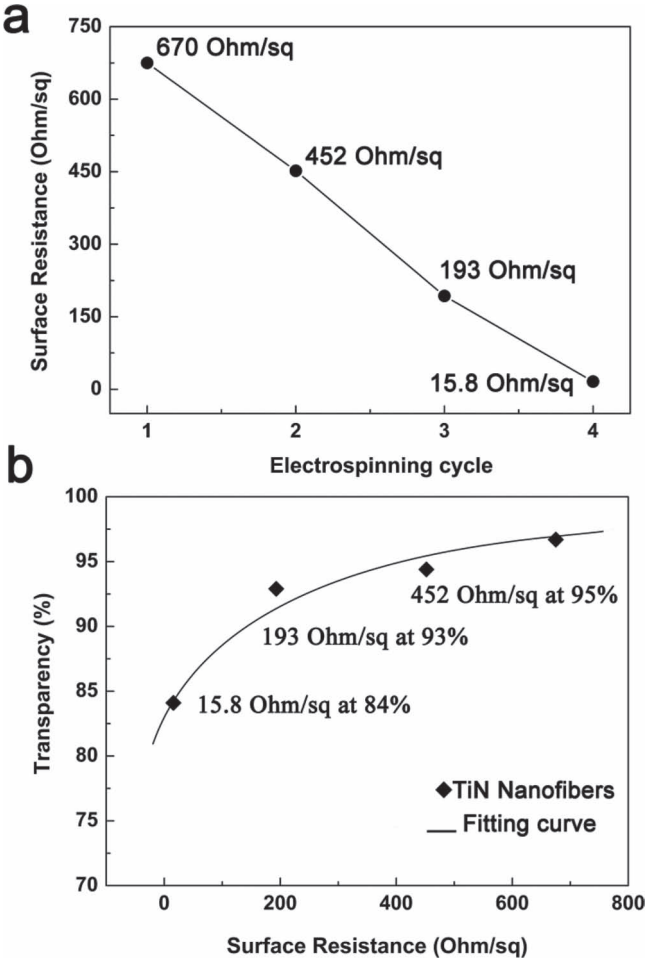

Figure 7. a) Sheet resistance of TiN nanofiber networks plotted as a function of electrospinning cycles. b) Transmittance at 550 nm vs sheet resistance for the TiN nanofiber networks deposited with different electrospinning cycles.

4. Experimental Section

Materials: PVP (MW = 1 300 000), ethanol, acetic acid, and tetrabutyl titanate were used as the starting materials.

Electrospinning: The synthesis procedure of TiO_2 nanofibers was similar to previous work. The tetrabutyl titanate was dissolved in an ethanol-acetic acid mixture. The PVP was added to the mixture to control the viscosity of the solution. After fully dissolution of PVP, the solution was delivered to a stainless needle at a constant flow rate of 1.0 mL h^{-1} by a peristaltic pump, with an aluminum foil placed 20 cm from the needle tip. The nanofibers were collected on the substrate by applying a high voltage of 20 kV.

Preparation of TiN Nanofibers: The precursor electrospun nanofibers were calcined at 500 °C in air for 2 h to obtain TiO_2 nanofibers. Afterword, the synthesized TiO_2 nanofibers were calcined in a tube furnace in ammonia atmosphere at various temperatures from 800 to 1100 °C. At the beginning of ammonification process, ammonia was flowed into the tube at a rate of 500 sccm for half an hour to expel the air in the tube. While maintaining the flowing ammonia of 120 sccm, the temperature was firstly increased from room temperature to 500 °C at a rate of 10 °C min^{-1}; then increased from 500 °C to 800, 900, 1000, 1100 °C at a rate of 5 °C min^{-1}, respectively; maintaining the temperature for 4 h afterward. The TiN nanofibers were obtained as the sample was allowed to cool to room temperature in ammonia atmosphere.

Characterization: The obtained nanofibers were characterized by means of scanning electron microscopy (SEM, LEO-1530, Carl Ziess Co., Oberkochen, Germany) and transmission electron microscopy (TEM, JEOL-2011, Tokyo, Japan). The phase constitution of the nanofibers was determined by X-ray diffraction using nickel-filtered CuKa radiation (XRD, D/max-2550, Rigaku Co., Tokyo, Japan). X-ray photoelectron spectroscopy (XPS, PHI-5300 ESCA, Michigan, U.S.A) was used mainly for the analysis of elemental and chemical states of N in the nanofibers. The current-voltage (*I–V*) characteristics of the TiN nanofibers were measured with a Keithley 4200 measurement system at room temperature. The sheet resistance measurements of TiN nanofiber networks were carried out by a four-probe method.

Supporting Information

Supporting Information is available from the Wiley Online Library or from the author.

Acknowledgements

This study was supported by the National Natural Science Foundation of China (Grant No. 50872063).

Received: April 8, 2012
Revised: June 8, 2012
Published online: August 17, 2012

[1] H. Hosono, H. Ohta, M. Orita, K. Ueda, *Vacuum* **2002**, *66*, 419.
[2] T. Minami, *Thin Solid Film* **2008**, *516*, 5822.
[3] A. Kumar, C. W. Zhou, *ACS Nano* **2010**, *4*, 11.
[4] K. S. Kim, Y. Zhao, H. Jang, S. Y. Lee, J. M. Kim, B. H. Hong, *Nature* **2009**, *457*, 706.
[5] Z. C. Wu, Z. H. Chen, X. Du, A. F. Hebard, A. G. Rinzler, *Science* **2004**, *305*, 1273.
[6] J. Li, L. Hu, L. Wang, Y. Zhou, G. Gruner, *Nano Lett.* **2006**, *6*, 2472.
[7] G. Eda, G. Fanchini, M. Chhowalla, *Nat. Nanotechnol.* **2008**, *3*, 270.
[8] M. Zhang, S. L. Fang, K. R. Atkinson, R. H. Baughman, *Science* **2005**, *309*, 1215.
[9] Y. L. Huang, A. Baji, H. W. Tien, Y. K. Yang, Y. W. Mai, N. H. Wang, *Nanotechnology* **2011**, *22*, 475603.
[10] L. Hu, D. S. Hecht, G. Gruner, *Nano Lett.* **2004**, *4*, 2513.
[11] Q. Yu, J. Lian, S. Siriponglert, H. Li, Y. P. Chen, S. S. Pei, *Appl. Phys. Lett.* **2008**, *93*, 113103.
[12] A. Reina, X. Jia, J. Ho, D. Nezich, H. Son, V. Bulovic, M. S. Dresselhaus, J. Kong, *Nano Lett.* **2009**, *9*, 30.
[13] H. Wu, L. B. Hu, M. W. Rowell, D. S. Kong, J. J. Cha, J. R. McDonough, J. Zhu, Y. Yang, M. D. McGehee, Y. Cui, *Nano Lett.* **2010**, *10*, 4242.
[14] P. Patsalas, S. Logothetidis, *J. Appl. Phys.* **2003**, *93*, 989.
[15] J. L. Gole, J. D. Stout, C. Burda, *J. Phys. Chem. B* **2004**, *108*, 1230.
[16] S. Sato, R. Nakamura, S. Abe, *Appl. Catal. A* **2005**, *284*, 131.
[17] R. Nakamura, T. Tanaka, Y. Nakato, *J. Phys. Chem. B* **2004**, *108*, 10617.
[18] R. Asahi, T. Morikawa, T. Ohwaki, *Science* **2001**, *293*, 269.
[19] H. Irie, Y. Watanaba, K. Hashimoto, *J. Phys. Chem. B* **2003**, *107*, 5483.
[20] H. Wu, D. D. Lin, R. Zhang, W. Pan, *J. Am. Ceram. Soc.* **2007**, *90*, 632.
[21] D. D. Lin, H. Wu, X. L. Qin, W. Pan, *Appl. Phys. Lett.* **2009**, *95*, 112104.
[22] D. D. Lin, H. Wu, R. Zhang, W. Pan, *Nanotechnology* **2007**, *18*, 465301.
[23] J. S. Im, S. J. Kim, P. H. Kang, Y. S. Lee, *J. Ind. Eng. Chem. (Amsterdam, Neth.)*. **2009**, *15*, 699.
[24] F. M. Du, J. E. Fischer, K. I. Winey, *Phys. Rev. B* **2005**, *72*, 121404.
[25] L. Hu, D. S. Hecht, G. Gruner, *Nano Lett.* **2004**, *12*, 2513.
[26] J. Y. Lee, S. T. Connor, Y. Cui, P. Peumans, *Nano Lett.* **2008**, *8*, 689.
[27] H. Wu, L. B. Hu, T. Carney, Z. C. Ruan, J. Zhu, S. H. Fan, Y. Cui, *J. Am. Chem. Soc.* **2011**, *133*, 27.
[28] L. B. Hu, H. S. Kim, J. Y. Lee, P. Peumans, Y. Cui, *ACS Nano* **2010**, *4*, 2955.